Point response characteristics for the CERES/EOS-PM, FM3 & FM4 instruments.

Jack Paden[*], G. Louis Smith[**], Robert B. Lee III[***], Dhirendra K. Pandey[*], Kory J. Priestley[***], Susan Thomas[*], and Robert S. Wilson[*]

*** Science Applications International Corporation**
One Enterprise Parkway, Suite 300
Hampton, VA 23666-5845

**** Thermal Radiation Group**
Department of Mechanical Engineering
Virginia Polytechnic Institute & State University
Blacksburg, VA 24061

*****Atmospheric Sciences Division**
NASA Langley Research Center, M.S. 420
Hampton, VA 23681-0001

ABSTRACT

This paper describes the point source functions (PSF's) of the Clouds and the Earth's Radiant Energy System (CERES,) Earth Observing System (EOS,) afternoon platform (PM,) Flight Model 3 (FM3,) and Flight Model 4 (FM4) scanning instruments. The PSF (also known as the Point Response Function, or PRF) is vital to the accurate geo-location of the remotely sensed radiance measurements acquired by the instrument. This paper compares the characteristics of the FM3 and FM4 instruments with the earlier Proto Flight Model (PFM) on the Tropical Rainfall Measuring Mission (TRMM) platform, and the FM1 and FM2 Models on the EOS morning orbiting (AM) platform, which has recently been renamed "Terra." All of the PSF's were found to be quite comparable, and the previously noted "spreading" characteristic of the window (water vapor) channel PSF is analyzed

Keywords: PSF, PRF, CERES, TRMM, EOS, Earth Radiation Budget

1. INTRODUCTION

The CERES/EOS-PM scanning radiometric measuring instruments are based on those which have been flown previously on the Earth's Radiation Budget Experiment (ERBE.) The CERES instruments measure three radiation wavelength bands: the total earth radiation (emitted and reflected) from 0.3 to >100 microns, the emitted "water vapor" window band from 8 to 12 microns, and the earth reflected shortwave radiation band from 0.3 to <5.0 microns. These bands were discussed by Barkstrom[1] in 1990. The Proto-Flight Model (PFM) of the CERES instrument is currently orbiting on the joint US/Japanese Tropical Rainfall Measuring Mission (TRMM) which was launched in November 1997. The Flight Model One (FM1) and Flight Model Two (FM2) instruments are both scheduled to orbit on the Earth Observation System (EOS) AM platform in

August 1999. Two additional CERES instruments (FM3 and FM4) are scheduled to be launched on the EOS-PM platform in 2001. A fifth instrument (FM5) awaits launch on a flight-of-opportunity (FOO.) The data acquired by these instruments is analyzed by computing radiation as measured by the CERES radiometer. These data will be compared to measurements acquired by higher resolution instruments such as the MODIS (Wielicki, et al.[2]). The Point Response Function (PRF) of the CERES measurements describe the response of the instrument to any point within the field-of-view. This response is determined by the instantaneous field-of-view, the time response of the detector and the signal conditioning filter (Smith[3]). The radiometric calibration facility (RCF) which was built for the CERES radiometer calibrations includes a PRF radiance source (PRFS). The beam of radiation from the PRFS source subtends a 0.17° cone, which is small compared to the instantaneous field-of-view (IFOV) of the radiometers; however, the finite solid angle of the beam must be considered in the data analysis. The Proto-Flight Model (PFM), Flight Model 1 (FM1), Flight Model 2 (FM2) instruments have previously been tested with the PRF source. Results for the TRMM instrument were discussed at SPIE's Aerosense97 Symposium in Orlando in 1997 (Paden[4]). Results for the EOS-AM, FM1 & FM2 instruments were discussed by Smith at SPIE's Symposium in San Diego in 1998 (Paden[5]) In this paper we discuss the analysis of the measurements for the FM3 and FM4 instruments, and their comparison with the previous instruments, and with the theoretical model developed by Smith[3].The results presented in this paper are compared to those acquired by the previous CERES instruments.

2. DESCRIPTION OF THE INSTRUMENT

Barkstrom[1] described the instruments used in the pioneering efforts to measure the Earth's outgoing radiation using remote sensing satellites. The CERES instrument, sensors, and RCF were described by Lee[6], et al. More recent descriptions of the pre-launch calibrations of the first three instruments were provided by Lee[7], et al. in the July 1998 IEEE Transactions, and by Paden[4,5], etal. at the SPIE Symposia in Orlando (1997) and San Diego (1998). Each CERES instrument (Fig. 1) has three scanning channels. The total channel is sensitive to radiation in the wavelength range of 0.3 to >100 microns; he window channel is sensitive to the (water-vapor) wavelengths from 8 to 12 microns; and the shortwave channel is sensitive to radiation in the 0.3 to 5.0 micron band. Each of the three bolometers is located at the focal plane of a Cassegrainian telescope (Fig. 2). The incident radiation is restricted by insertion of a FOV limiter in the shape of an elongated hexagon (Fig. 3) in the optical path. The instrument is capable of slewing in both azimuth and elevation, and can be operated while scanning with either a fixed or rotating azimuth plane.

3. THE THEORETICAL PSF MODEL

The modified Smith[3] theoretical model used for the analysis of data from the point response function source (PRFS) has been thoroughly discussed in previous papers by Paden[4,5], and will not be repeated here. The ground calibration data for all previous CERES instruments were analyzed using laborious, and somewhat error-prone, manual methods. The potential for error was primarily due to the large numbers of files involved (40 to 50); the fact that 4 scans, in opposite directions, were made across the PRFS source in each record; the fact that 3 different azimuthal offsets were associated with each scan-normal test; and human fallibility. The PRFS data for the FM3 and FM4 instruments were analyzed using an automated program written in the Research Systems, inc. (RSI) Interactive Data Language (IDL®,) The program is designed to eliminate the human fallibility factor by insuring that the repetitive operations necessary to temporally and spatially shift the PRFS off-azimuth data are completed in the same manner on each data file analyzed.

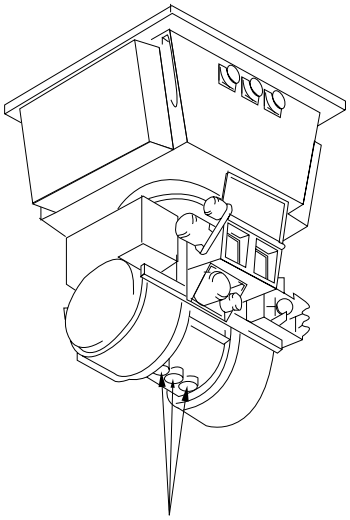

Figure 1. CERES Scanner Instrument

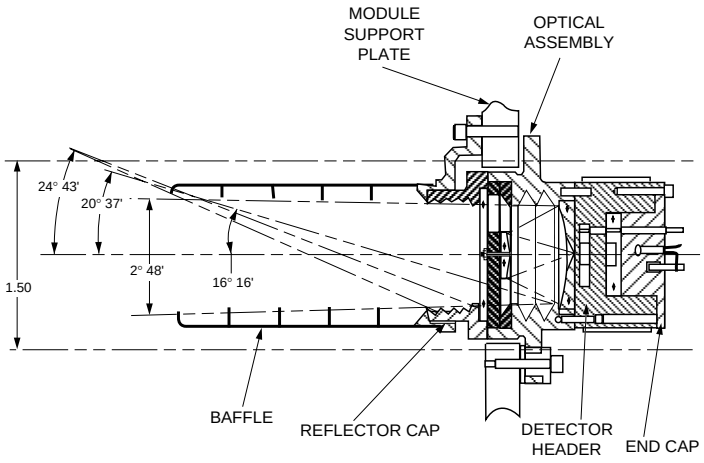

Figure 2. CERES Telescope Design

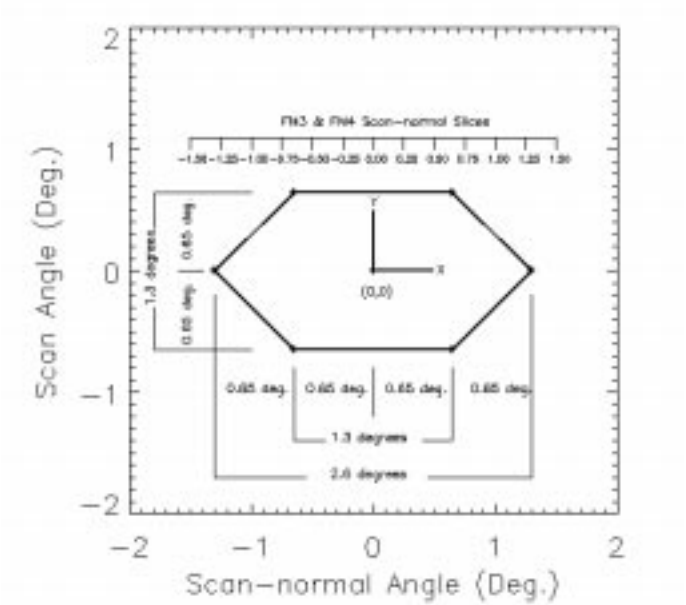

Figure 3. FOV Limiter & Scan Paths for FM3 & FM4

.

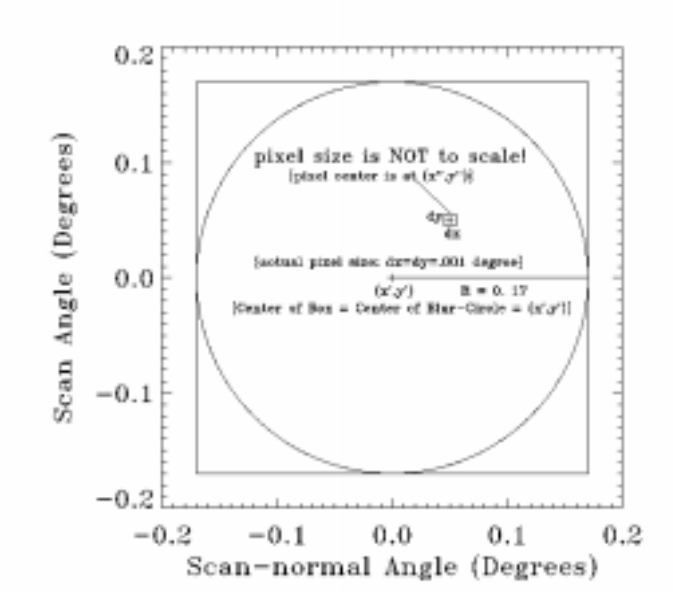

Figure 4. PSF Blur-Circle Integration

In this study, the modified Smith model was used to generate a finite source response contour for the CERES/EOS-PM instruments (designated as FM3, and FM4 respectively), using their measured detector time constants. The Smith[3] model was supplemented by adding code which assumes a circular, finite source emitting exactly 1 unit of radiance uniformly over its entire surface, moving across the FOV of the detector (Fig. 4)

4. DESCRIPTION AND ANALYSIS OF DATA

The measurements used in this comparison were acquired by TRW personnel at their Radiometric Calibration Facility (Fig. 5) in Redondo Beach, California. The instruments tested were the FM3 and FM4 models of the CERES scanning radiometer which are scheduled to be launched aboard the EOS-PM platform in November 1999. In the RCF, the instruments are mounted with their scan axes in the vertical direction (the scan plane is therefore horizontal.) During testing, the FM3 and FM4 instruments executed the scan profiles described in Table 1, and graphically depicted in Figure 6. The two different profiles were occasioned by the fact that the scan-rate for FM4 was increased (from the 62.96 degrees/second rate used for the PFM, FM1, FM2, and FM3) to 66.99 degrees per second, in order to prevent source saturation of the total and shortwave channel detectors. Analysis of the data determined the location of the PRFS within the RCF scan plane. [90.26 degrees instrument scan elevation angle for the FM3 (Fig. 7) and 94.7. degrees for the FM4 (Fig. 8) EOS-PM instruments.] The source beam was rotated normal to the scan direction from -1.5 degrees to +1.5 degrees in 0.25 degree increments. At each of the scan-normal angles; 3 files each, containing between 10 and 20 records; and each record containing 660 samples of data, were acquired. All of the data in each file was corrected for drift and offset, and all resulting files were averaged to produce a single record representing the aggregation of all data in the set. Each averaged 660 sample record contained two alternating, backward and forward scans across the source at the CERES PRFS scan rate. Because of the backward and forward scan pattern the leading edge of the finite source will allow radiance to impinge on the detector exactly 1.3 degrees (the width of the FOVL) in angle earlier on the backward scan than on the forward scan. One file (of the set of 3) was recorded with the source pointed directly at the instrument(i.e., 0 degree cant in the scan angle); another was recorded with the source canted -0.2 degrees in the scan angle plane; and the third file was recorded with the source canted +0.2 degrees in the scan angle plane. This canting was necessary since, at the PRFS scan rate, and a sampling rate of 0.01 second, data points are spaced approximately 0.6 degrees, and canting the source by 0.2 degrees in each direction provides data points approximately every 0.2 degrees. Merging the data from the three files has the effect of providing “apparent” sampling within FOV limits, at a rate of 3-times the true rate, thus allowing us to

more accurately characterize the shape of the response signal within the FOVL. For the 0 degree scan angle cant file, no time correction was needed. However, due to the four scans over the source in each file, the ±0.2 degree cant files required four time corrections in each record to account for the alternating lead/lag due to the cant angle. The three resultant averaged files (+0.2 degree, 0 degree, and -0.2 degree cant) for each scan-normal angle were then appended onto one file and time sorted, thus producing a 1980 sample file representing the “enhanced” scan record. One should note that the “enhanced” scan record is NOT evenly sampled due to the 0.01 second basic sampling rate coupled with the 0.2 degree deflection of the PRFS beam.

Graphical displays of data acquired for the FM3 and FM4 total channels are shown in Figs. 7 & 8, respectively The scan rate for the FM4 tests was increased from 62.96 to 66.99 degrees per second. The apparent sampling intervals for the FM3 instrument were 3.176, 3.176, and 6.824 milliseconds; and for the FM4 instrument they were 2.986, 2.986, and 5.972 milliseconds. The scan rate was increased (by TRW) to insure that the detectors were not saturated by the source, the radiant energy output of which had increased significantly over that for FM3. These particular sets of data apply only to the 0 degree scan-normal angle where the finite source passes through the geometric center of the FOV, but they are illustrative of all of the other PSF data sets used in this analysis. For each of the data sets, and for each scan-normal position, the four scans across the PRFS source were “initialized” at the leading edge of the FOV (i.e., time = 0 when the first pixel passes ±0.65 degrees on the scan axis,) and the resultant data set was again averaged. The aggregation of all of these data sets provided the input for the contour plots of the PSF.

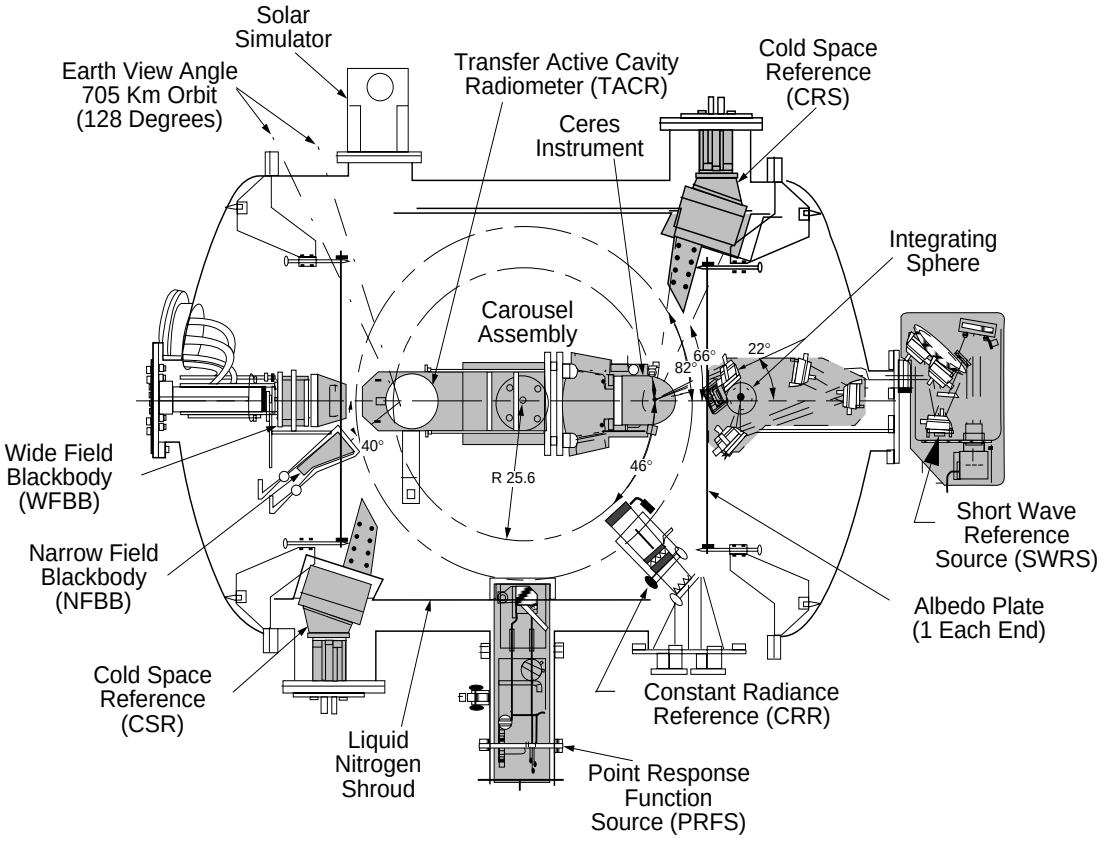

Figure 5. Radiometric Calibration Facility

Table 1: EOS-PM Scan Profile

Scan Angle (degrees)	Time (seconds) FM3	Time (seconds) FM4
107	0.00	0.00
107	0.84	0.84
73	1.38	1.35
73	1.94	1.94
107	2.48	2.45
107	4.14	4.14
73	4.68	4.65
73	5.24	5.24
107	5.78	5.75
107	6.59	6.59

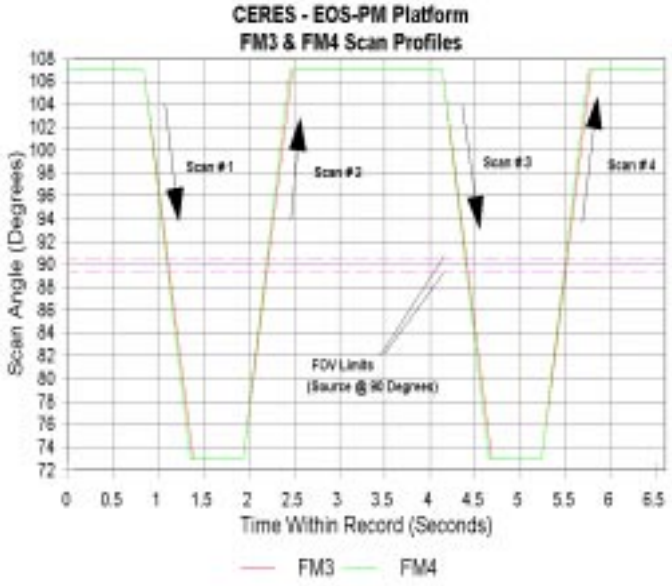

Figure 6. PRFS Data Collection Patterns

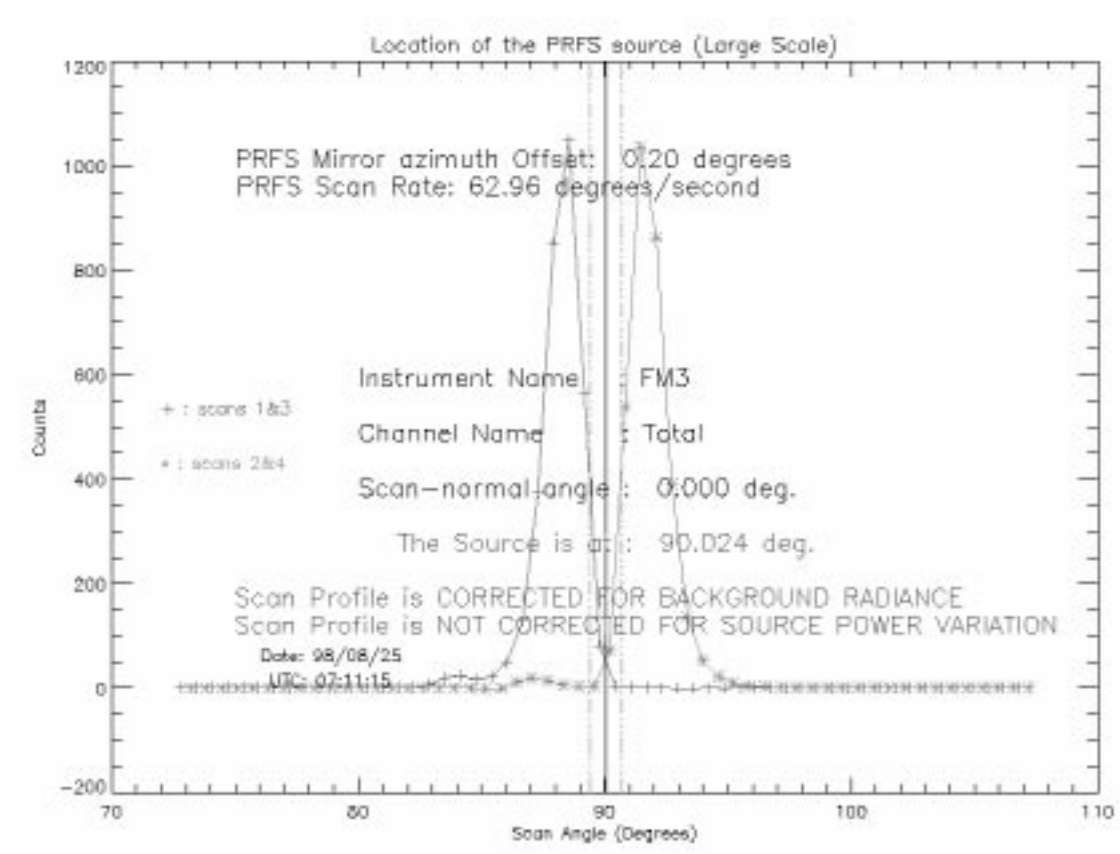

Figure 7. FM3 Total Channel PRFS Scans (Mid-FOVL)

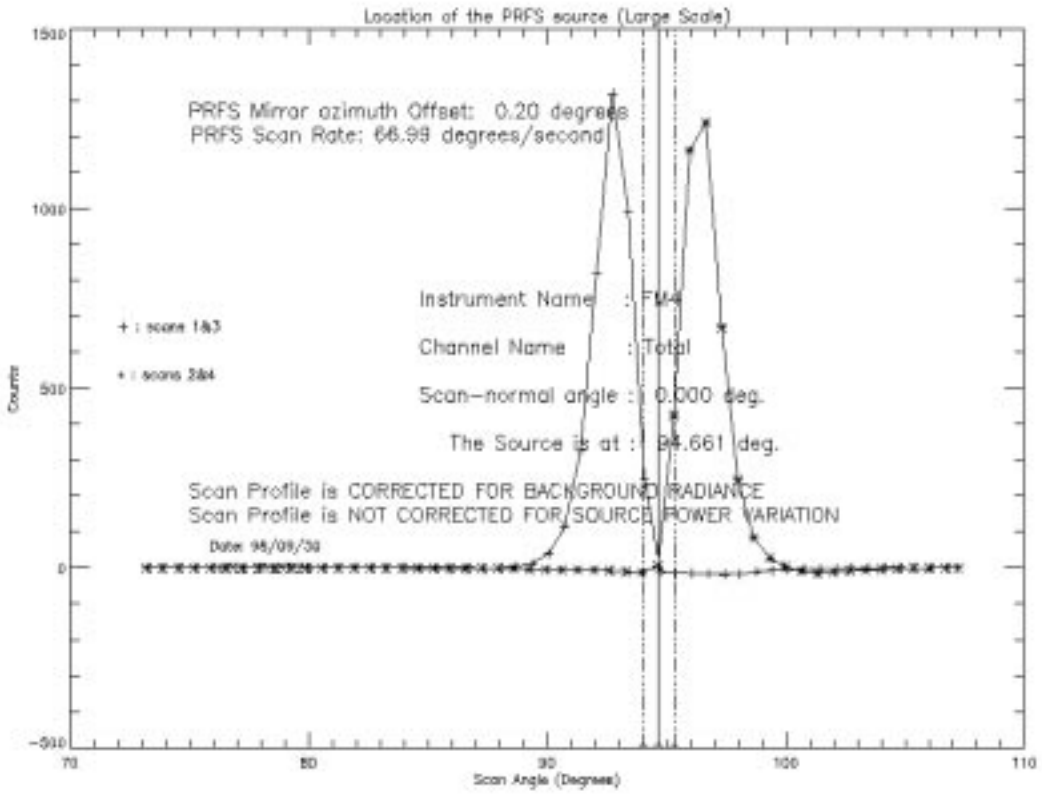

Figure 8. FM4 Total Channel PRFS Scans (Mid-FOVL)

Because of the time-span of the measurements for the various scan-normal positions, the PRFS source intensity varied quite a bit over the time intervals involved. Source intensity was not monitored directly, but rather by recording data at the central FOVL position several times throughout the data acquisition process. During our analysis, the application of linearly interpolated power correction adjustments was not found to be helpful, so we did not use it in this analysis

The finite source model was executed using an effective source radius of 0.17 degree. The pixel size used was 0.001 of a degree, which provides 340 pixels (Fig. 4) across the blur circle and limits the possible error in radiance calculations to no more that 0.00774%. For this radius and pixel size, there were 90785 (counted) pixels in the full blur circle. The comparative results of the modeling and measurement efforts for the FM3 instrument are displayed in six figures; figures 9-11showing results for the finite source (radius = 0.17) model; and figures 12-14 showing plots of the “normalized” measured data. The comparable results of the modeling and measurement efforts for the FM4 instrument are displayed in six figures; figures 15-17 display results for the finite source (radius = 0.17) model; and figures 18-20 display plots of the “normalized” measured data. An image of the FOV limiter has been superimposed on all plots for reference. By normalized we mean that the measured data was scaled so that its maximum is equal to the maximum value in the *modeled* data and thus direct visual comparison of equivalent contour intervals can be easily made.

5. ANALYSIS OF THE RESULTS

Figures 7 & 8 indicate that there was a slight attenuation of the detected radiance in the “back-scan” direction, and this characteristic was noted in all previous CERES instruments. In the process of “normalizing” the scans, these differences were averaged out. The source of these differences is not known. The comparisons of the modeled and measured total contours are excellent; and the shortwave channel comparisons are very good There is a significant spread of contours in the scan direction for the measured window channel data when background radiance compensation is not considered. Priestley (1997) suggested that the spread was probably due to the relatively small signal-to-noise ratio for the window channel, and that by removing the “background” radiance we would thereby minimize the spread.

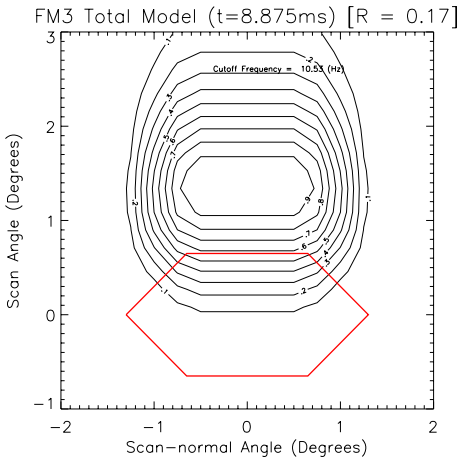

Figure 9. FM3 Total Modeled PSF

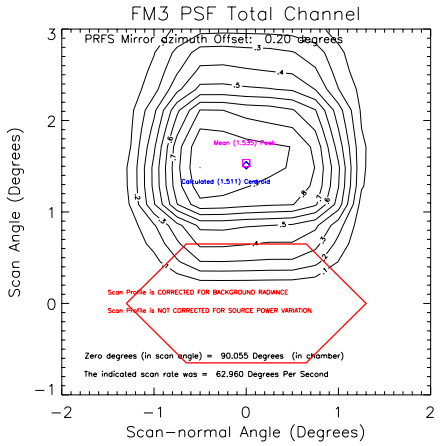

Figure 12. FM3 Total Measured PSF

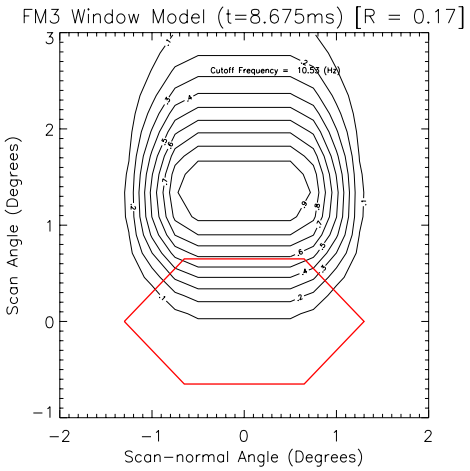

Figure 10. FM3 Window Modeled PSF

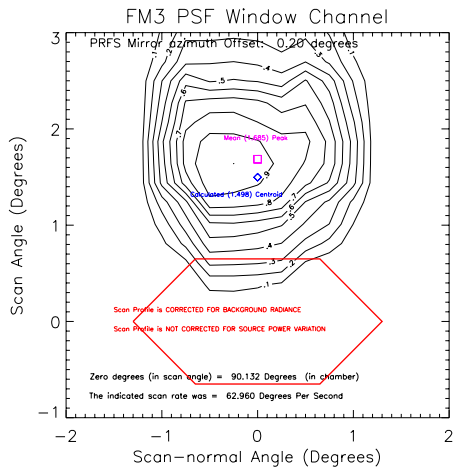

Figure 13. FM3 Window Measured PSF

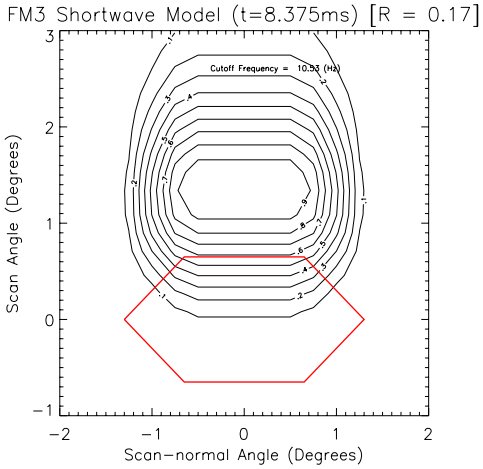

Figure 11. FM3 Shortwave Modeled PSF

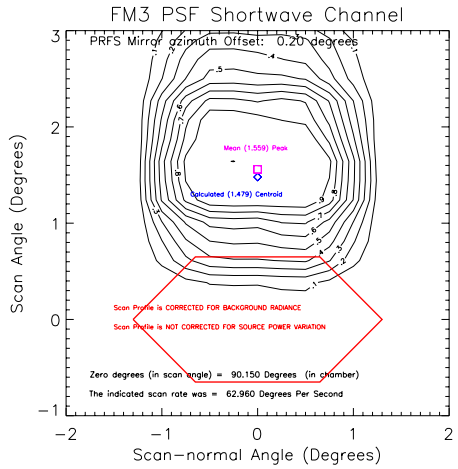

Figure 14. FM3 Shortwave Measured PSF

Figures 9 through 14. CERES FM 3 Instrument Contours

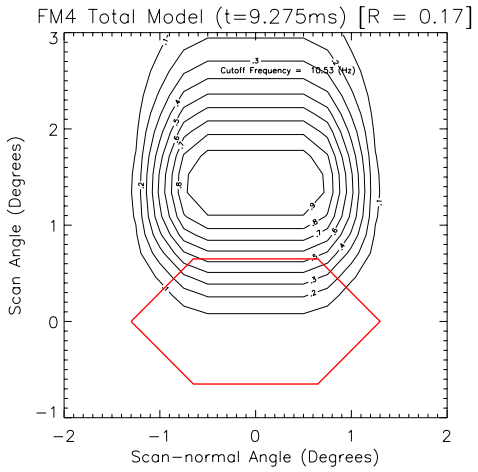

Figure 15. FM4 Total Modeled PSF

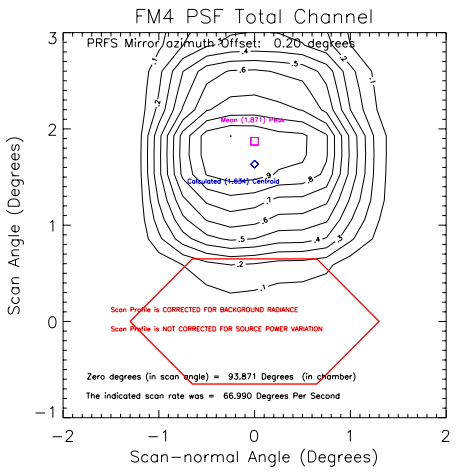

Figure 18. FM4 Total Measured PSF

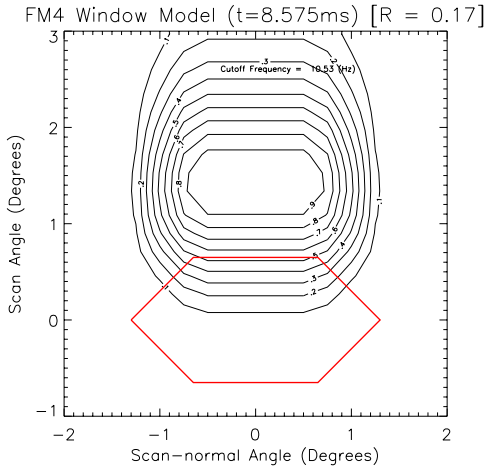

Figure 16 FM4 Window Modeled PSF

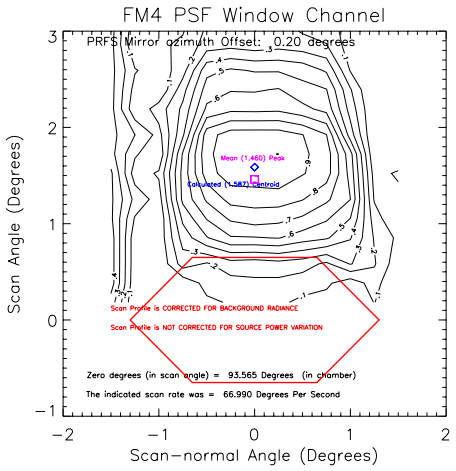

Figure 19. FM4 Window Measured PSF

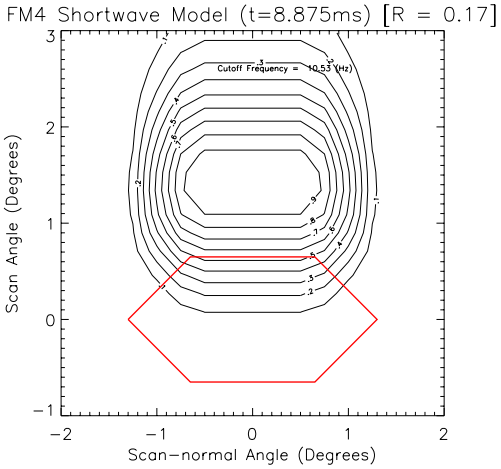

Figure 17. FM4 Shortwave Modeled PSF

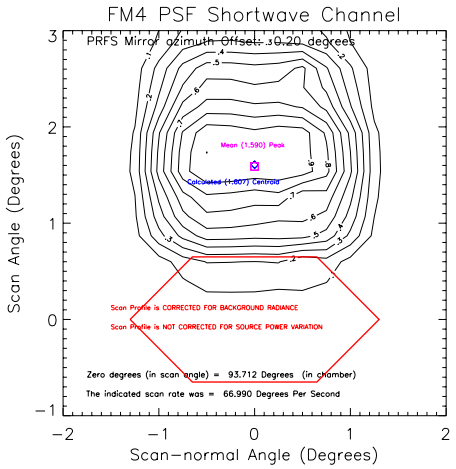

Figure 20. FM4 Shortwave Measured PSF

Figures 15 through 20. CERES FM4 Instrument Contours

6. CONCLUDING REMARKS

We have demonstrated here (and in previous discussions[4,5]) that the modified PSF model accurately predicts the experimentally measured contours of the CERES scanning radiometers. Based on the tests performed using the finite source model, the differences between the modeled and measured values are very small for the total and shortwave channels., and the spreading of the measured window channel contours (with respect to the modeled data) can be compensated by removing the ambient background radiance as suggested by Priestley. The relatively low level of the window channel signal compared to the thermal gradients proximal to the PRFS source (Fig. 21) do indeed appear to have been the primary reason for the window channel contour spread (Fig. 22.) Figures 23 & 24 show the corresponding contour response to the removal of background signal.

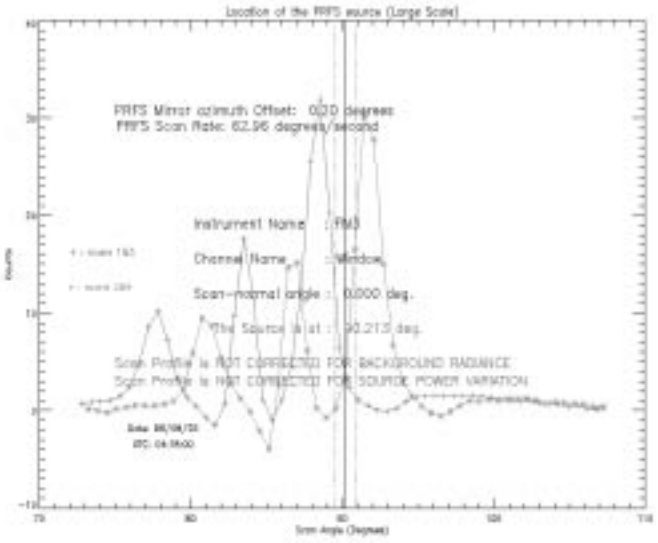

Figure 21. Window Channel w/background

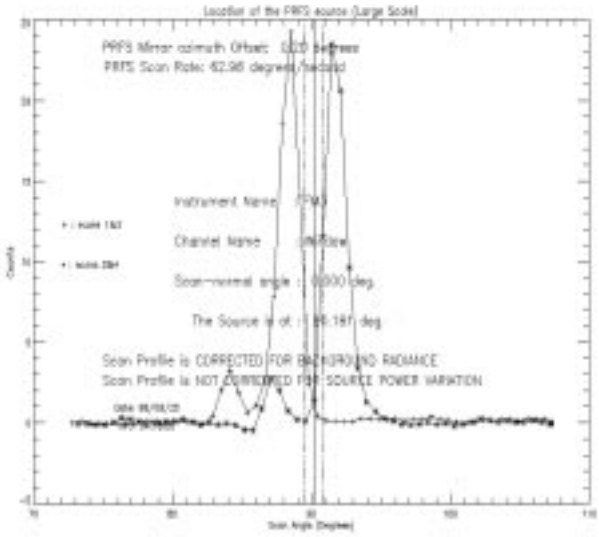

Figure 22. Window Channel wo/background

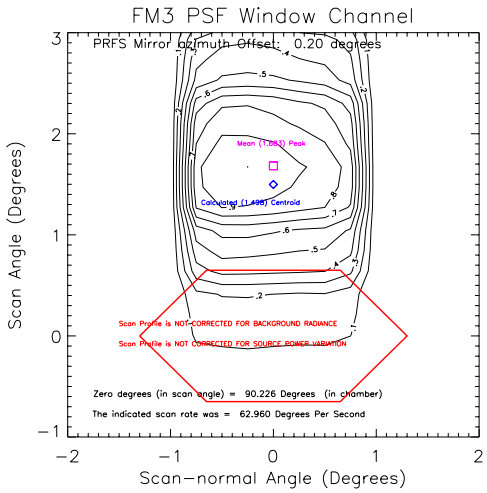

Figure 23. Window Channel w/Background

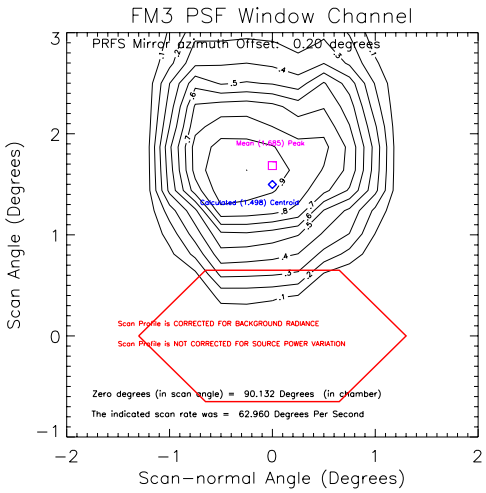

Figure 24. Window Channel wo/Background

Figures 21 through 24. Window Channel Comparisons (with & without background radiance)

A comparison of the results of testing for the FM3 and the FM4 CERES instruments with the results obtained from the PFM, FM1, and FM2 testing, shows very good agreement in all three channels. The spread in the window channel persists for all 5 instruments, but is compensated when the effects of background radiation is taken into account (FM3 and FM4 instruments). The intercomparison of the three instruments shows that they are all very consistent in their contour patterns, and they all have essentially the same delay characteristics.

The good news is that all five CERES instruments exhibit essentially the same PSF characteristics. A tabulation of the offsets of the peak radiance measurements from the optical axis is shown in Table 2, along with the calculated centroid of the theoretical PSF. All tabulated values are in degrees. Note that the increased scan rate for FM4 moves the calculated centroid farther away from the optical axis because the centroid location is directly proportional to the scan rate.

Table 2: CERES radiance peaks & centroidal offsets from the optical axis (in degrees)

CERES Instrument	Total Channel		Window Channel		Shortwave Channel	
	Radiance Peak	Calculated Centroid	Radiance Peak	Calculated Centroid	Radiance Peak	Calculated Centroid
PFM	1.686	1.493	1.636	1.475	1.626	1.465
FM1	1.622	1.487	1.694	1.453	1.595	1.471
FM2	1.496	1.456	1.464	1.468	1.444	1.468
FM3	1.535	1.511	1.684	1.498	1.559	1.479
FM4	1.871*	1.634*	1.460*	1.587*	1.590*	1.607*

*: The FM4 PRFS scan rate was 66.99 deg/sec vs. 62.96 deg/sec for PFM through FM3

ACKNOWLEDGEMENTS

The measurements used in this paper were acquired by TRW personnel at their Radiometric Calibration Facility in Redondo Beach, California. We wish to thank them for their efforts; in particular, Steve Carman, Project Manager; Peter Jarecke, Assistant Project Manager for Calibration, who designed the Radiometric Calibration Facility; Mark Frink, who designed the Point Response Function Source; Herb Bitting, who provided most of the data files and associated calibration test reports necessary to produce the contour plots in this paper; and Tom Evert, who provided information on the scan rate change for FM4. This work was partially funded under NASA Contract NAS 1-19570 with the NASA Langley Research Center, Hampton, Virginia.

REFERENCES

1. B. R. Barkstrom, “Earth radiation budget measurements: pre-ERBE, ERBE, and CERES,” in *Long-term Monitoring of the Earth’s Radiation Budget*, B. R. Barkstrom, ed. **Proc. Soc. Photo-Opt. Instrum. Eng., 1299**, 52-60 (1990).

2. B. A. Wielicki., B. R. Barkstrom, E. F. Harrison, R. B. Lee III, G. L. Smith, and J. E. Cooper: "Clouds and the Earth's Radiant Energy System (CERES): An Earth Observing System Experiment," **Bull. Amer. Met. Soc.**, **77**, 853-868 (1996).

3. G. Louis Smith, “Effects of time response on the point spread function of a scanning radiometer,” **Applied Optics**, **33**, pages 7031-7037 (1994).

4. J. Paden, G. Louis Smith, Robert B. Lee III, D. K. Pandey, Kory J. Priestley, Herbert Bitting, and Susan Thomas, “Reality Check: a point response function (PRF) comparison of theory to measurements for the Clouds and the Earth’s Radiant Energy System (CERES) Tropical Rainfall Measuring Mission (TRMM) instrument”, **Proc. Soc. Photo-Instrum. Eng.,** Vol. 3074, pages 109-117, (1997).

5. J. Paden, G. Louis Smith, Robert B. Lee III, D. K. Pandey, Kory J. Priestley, Herbert Bitting, Susan Thomas, and Robert S. Wilson, “Comparisons between Point Response Function measurements and theory for the Clouds and the Earth’s Radiant Energy System (CERES) TRMM and the EOS-AM spacecraft thermistor bolometer sensors”, **Proc. Soc. Photo-Instrum. Eng.,** Vol. 3439, pages 344-354, (1998).”

6. R. B. Lee III, B. R. Barkstrom, G. Louis Smith, J. H. Cooper, L. P. Kopia, and R. W. Lawrence, “The Clouds and the Earth’s Radiant Energy System (CERES) Sensors and Preflight Calibration Plans”, **Journal of Atmospheric and Oceanic Technology**, **13**, pages 300-313 (1996).

7. R. B. Lee III, Bruce R. Barkstrom, Herbert C. Bitting, Dominique A. H. Crommelynck, Jack Paden, Dhirendra K, Pandey, Kory J. Priestley, G. Louis Smith, Susan Thomas, K. Lee Thornhill, and Robert S. Wilson, “Prelaunch Calibrations of the Clouds and the Earth’s Radiant Energy System (CERES) Tropical Rainfall Measuring Mission and Earth Observing System Morning (EOS-AM1) Spacecraft Thermistor Bolometer Sensors”, **IEEE Transactions on Geoscience and Remote Sensing,** Vol. 36, No. 4, July 1998.

8. P. Jarecke and S. Carman, “CERES PFM/TRMM Instrument Calibration FInal Test Report”, **TRW DRL 37.5, 55067.600.010,** 11 December 1995.

9. H. Bitting and S. Carman, “CERES EOS AM-1 Flight Model 1 Calibration Test Report”, **TRW DRL 38.5, 55067.600.013,** 16 May 1997.

10. H. Bitting and S. Carman, “CERES EOS AM-1 Flight Model 2 Calibration Test Report”, **TRW DRL 38.5, 55067.600.014,** 25 June 1997.

Further Author Information -
Jack Paden: E-mail; j.paden@larc.nasa.gov; Telephone: 757-827-4880; Fax: 757-825-9129.
G. Louis Smith: E-mail: lou@vger.nasa.gov; Telephone: 757-864-5678; Fax: 757-864-7996.
Robert B. Lee: E-mail: r.b.lee@larc.nasa.gov; Telephone: 757-864-5679; Fax: 757-864-7996
D. K. Pandey: E-mail: d.k.pandey@larc.nasa.gov; Telephone: 757-827-4890; Fax 757-825-9129.
Susan Thomas: E-mail: s.thomas@larc.nasa.gov; Telephone: 757-827-4879; Fax: 757-825-9129.
Kory J. Priestley: E-mail: k.j.priestley@larc.nasa.gov; Telephone; 757-864-8147; Fax 757-864-7996.
Robert S. Wilson: E-mail: r.s.wilson@larc.nasa.gov; Telephone: 757-827-4881; Fax 757-825-9129.